Modeling of photovoltaic systems and parameter extraction using the ant colony optimization algorithm

Arlon Natã Alves Granja Delmondes[1], Luis Arturo Gómez-Malagón[1]

1 University of Pernambuco, Polytechnic School of Pernambuco, 50720-001, Recife, PE, Brazil

Summary

Accurate extraction of electrical parameters from photovoltaic (PV) cell models is essential for the simulation and performance optimization of solar energy systems. This study introduces a hybrid algorithm based on Ant Colony Optimization (ACO), enhanced with a local search mechanism and a reduced search-space strategy, for parameter extraction in the single-diode (SDM) and double-diode (DDM) models. Using a publicly available experimental dataset from a commercial silicon PV cell (R.T.C. France, under 1000 W/m² irradiance and 33 °C), the proposed algorithm was implemented and validated. The method exhibited high accuracy, achieving Root Mean Square Error (RMSE) values of 1.930×10^{-3} for the SDM and 2.777×10^{-3} for the DDM. A comprehensive statistical analysis over 30 independent runs demonstrated that the proposed hybrid ACO algorithm provides strong consistency (standard deviation $\approx 6.0 \times 10^{-6}$ for SDM and 9×10^{-6} for DDM) and rapid convergence for both SDM and DDM models (5 iterations for SDM and 11 iterations for the DDM to achieve a RMSE = 5×10^{-3}). Compared with well-established metaheuristics such as Particle Swarm Optimization (PSO) and Genetic Algorithm (GA), the proposed approach proved to be a highly reliable and computationally efficient alternative for PV parameter estimation and system modeling.

Keywords: Optimization, modeling, PV system, parameters, Ant colony optimization

1. Introduction

The global transition towards sustainable energy sources is heavily reliant on the advancement of renewable technologies, with photovoltaic (PV) systems playing a central role. To ensure the efficiency, optimal design, and accurate performance assessment of these systems, the use of mathematical models that describe their electrical behavior under varying operational conditions is imperative. Modeling, based on equivalent circuits, allows for the simulation of the characteristic Current-Voltage (I-V) curve of a PV module (Fahim et al., 2022).

Among the existing equivalent circuit models, the Single-Diode Model (SDM) is widely utilized for its effective balance between simplicity and accuracy. To capture recombination losses in the depletion region, especially under low irradiance, the Double-Diode Model (DDM) is frequently employed (Ishaque et al., 2011). Recent literature also explores the Three-Diode Model (TDM), which offers even higher precision by accounting for losses caused by defects in the crystal structure of the cell and at the grain boundaries, albeit at the cost of increased computational complexity and the need to extract a larger set of parameter (Fahim et al., 2022; Bakır, 2023).

The effectiveness of these models is contingent upon the accurate extraction of their intrinsic parameters (e.g., photocurrent, series and shunt resistances, and diode ideality factors), a process widely recognized as a critical issue for the simulation and evaluation of PV systems. This parameter identification constitutes a complex and non-linear process, for which traditional approaches can be insufficient. Consequently, various metaheuristic algorithms have been successfully applied to solve this problem. Techniques such as Particle Swarm Optimization (PSO), Genetic Algorithms (GA), and Simulated Annealing (SA) are frequently cited in the literature and have demonstrated robustness in the search for optimal solutions across numerous comparative studies (Louzazni et al., 2018).

In the relentless pursuit of enhancing parameter extraction, researchers have explored an extensive array of innovative metaheuristics. For example, Xiong et al. (2018) proposed an Improved Whale Optimization Algorithm (IWOA), demonstrating that enhancing existing algorithms can lead to superior performance over

10.18086/swc.2025.03.45 Available at http://proceedings.ises.org

their original versions. Similarly, other nature-inspired techniques have been successfully applied; a comparative analysis by Bakır (2023) included the Grey Wolf Optimizer (GWO), while Messaoud (2020) demonstrated the effectiveness of the Ant Lion Optimizer (ALO).A comprehensive review by Fahim et al. (2022) cataloged dozens of such algorithms, highlighting a clear trend in the field towards hybrid methods. These advanced approaches often combine the strengths of different optimizers or integrate local search mechanisms to enhance exploitation, justifying the direction of the present work. Despite the success of several techniques, Ant Colony Optimization (ACO)—a metaheuristic inspired by the foraging behavior of ants and known for its effective balance between exploration and exploitation of the search space—remains comparatively less explored for this specific application. Therefore, the objective of this work is to develop and validate a hybrid ACO algorithm for the parameter extraction of the SDM and DDM. By leveraging a reduced search space strategy and a local search mechanism, this study aims to demonstrate that the proposed method offers superior robustness and efficiency when compared to other established metaheuristics, validating its potential as a highly reliable tool for photovoltaic modeling.

2. Methodology

This section details the mathematical models used to represent the photovoltaic cell, the formulation of the optimization problem, the architecture of the proposed algorithm for parameter extraction, and the experimental setup for validation.

2.1 Mathematical Modelling of Photovoltaic Cells

Equivalent circuit models commonly represent the non-linear relationship between the current and voltage of a photovoltaic cell. These models are essential for accurately simulating the I-V characteristic curve under various operating conditions. In this work, the single-diode (SDM), double-diode (DDM) models were considered to provide a comprehensive framework.

2.1.1 Single-Diode Model (SDM)

The SDM (figure 1 - A) is the most widely used model due to its effective balance between simplicity and accuracy. It represents the PV cell as a photocurrent source (I_{ph}) in parallel with a single diode and a shunt resistance (R_{sh}) all in series with a resistance (R_s).

The implicit equation governing the output current (I_{pv}) as a function of the output voltage (V_{pv}) is given by (Fahim et al., 2022):

$$I_{pv} = I_{ph} - I_s \left(e^{\left(\frac{V_{pv}+I_{pv}\cdot R_S}{n\cdot V_t}\right)} - 1 \right) + \frac{V_{pv}+R_S\cdot I_{pv}}{R_{sh}} \qquad \text{(eq.1)}$$

where I_{ph} represents the photocurrent, I_s is the reverse saturation current of the diode, n is the diode ideality factor and V_t is the thermal voltage, defined as $V_t = kT/q$, where k is the Boltzmann constant, T is the cell temperature in Kelvin, and q is the elementary charge. The extraction process for this model involves identifying five unknown parameters: I_{ph}, I_s, R_s, R_{sh} and n.

2.1.2 Double- Diode Model (DDM)

To capture recombination effects, the DDM (Figure 1 - B) adds a second diode. This model is frequently employed to address recombination losses in the depletion region, especially under low irradiance conditions, where the Single-Diode Model (SDM) might not be as accurate (Ishaque et al., 2011).

The modelling of the DDM is given by:

$$I_{pv} = I_{ph} - I_{s1} \left[e^{\left(\frac{V_{pv}+I_{pv}\cdot R_S}{n1\cdot V_t}\right)} - 1 \right] - I_{s2} \left[e^{\left(\frac{V_{pv}+I_{pv}\cdot R_S}{n2\cdot V_t}\right)} - 1 \right] - \frac{V_{pv}+R_S\cdot I_{pv}}{R_{sh}} \qquad \text{(eq.2)}$$

Where I_{s1} and I_{s2} are the reverse saturation currents of diodes 1 and 2, respectively and n_1 and n_2 are the ideality factors of diodes 1 and 2.

This model requires extraction of seven parameters: I_{ph}, I_{s1}, I_{s2}, n_1, n_2, R_{sh} and R_s.

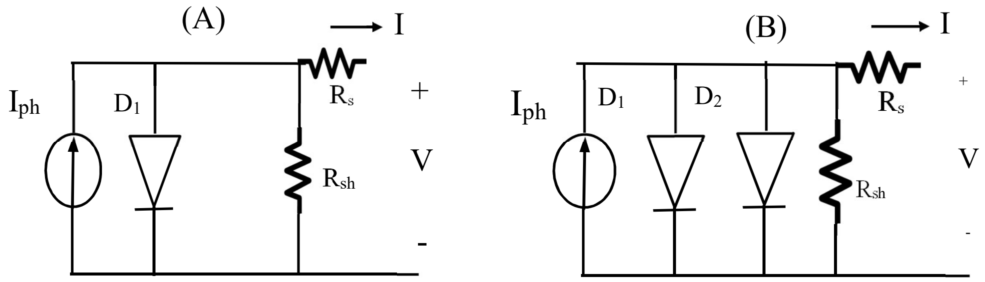

Figure 1: (A) Single diode and (B) Double diode circuit

2.2. Problem Formulation

The optimization for the extraction of parameters of a photovoltaic cell/module aims to minimize the error between a current-voltage (I-V) curve from a measured database and the curve calculated from the SDM and DDM using the extracted parameters. While several error metrics are used in the literature to serve as the objective function for this task, such as the Mean Absolute Error (MAE) and the Sum of Squared Errors (SSE) (Fahim et al., 2022; Louzazni et al., 2018), the Root Mean Square Error (RMSE) was chosen because it is a standard benchmark in the field and it gives a higher weight to larger errors by squaring the deviations before averaging. These characteristics favors solutions that maintain a consistently close fit across the entire I-V curve, avoiding large individual point errors (Bakır, 2023). The objective function is therefore defined as:

$$RMSE = \sqrt{\frac{1}{N}\sum_{i=1}^{N}((I_{real} - I_{estimated})^2)} \quad \text{(eq. 3)}$$

Where N is the total number of measured data points, and I_{real} and $I_{estimated}$ are the measured and estimated currents, respectively. The optimization process is subject to the physical boundary constraints (lower and upper bounds) for each parameter, as defined in the experimental setup.

2.3 Ant Colony Optimization (ACO)

2.3.1 Principles of Ant Colony Optimization

The Ant Colony Optimization (ACO) metaheuristic, introduced by Dorigo and Di Caro (1999), is a swarm intelligence technique inspired by the foraging behavior of ants. In its original formulation for discrete optimization problems (e.g., the Traveling Salesman Problem), the method uses a population of *Num_ants* (Number of Ants) to build solutions by moving on a graph.

The movement of the ants is probabilistic and guided by two main components: the pheromone trail (τ_{ij}) and a heuristic value (n_{ij}). The probability (ρ_{ij}) of an ant at node *i* choosing to move to the next node *j* is given by the classical ACO probability rule:

$$\rho_{ij} = \frac{[\tau_{ij}]^{\alpha} x [n_{ij}]^{\beta}}{\sum_{k \in allowed}[\tau_{ik}]^{\alpha} * [n_{ik}]^{\beta}} \quad \text{(eq. 4)}$$

where α (Alpha) is the Pheromone Weight, controlling how much the existing pheromone trail influences the decision. β (Beta) is the Heuristic Weight, controlling how much the priori heuristic information influences the decision, and $allowed$ is the set of allowed next nodes.

After all ants build their solutions, the pheromone trails are updated. This involves Pheromone Evaporation, where all trails are uniformly reduced by a rate ρ (Rho) to encourage exploration, followed by Pheromone Deposition, where ants that found good solutions reinforce desirable paths.

Since the parameter-extraction problem resides in a continuous search space, the classical discrete ACO framework must be reformulated. In continuous ACO, the notion of "paths" in a graph is replaced by sampling from a probability density function (PDF), typically a Gaussian distribution, which reflects the pheromone model over continuous parameters. For example, in the continuous-domain ACO extension by SamACO:

Variable Sampling Ant Colony Optimization Algorithm for Continuous Optimization (Hu et al., 2010) each decision variable is sampled from a Gaussian kernel whose shape is influenced by pheromone intensity.

In this work the classical ACO was adapted to continius domain as follows:

- Initialization: A new generation of N_{ants} (Num_ants) solutions is created where each ant X_i is a vector of parameter, randomly generated within their boundary constraints. The pheromone trails τ_j for each *j-th* parameter are also initialized to a uniform value.
- Fitness Evaluation: At the start of each iteration, the fitness of every ant in the population is evaluated by calculating its RMSE. The algorithm then identifies and stores the X_{best} (Global Best Solution), which is the solution vector with the lowest RMSE found across all iterations thus far
- Stopping criterion: The algorithm checks if the current iteration count has reached the predefined *Max_iter*. If this condition is met, the process terminates and outputs the X_{best} solution. If not, the iteration continues.
- Evaporation: To prevent premature convergence, all pheromone trails are uniformly reduced by an evaporation rate *rho* $\rho \in [0; 1]$ $(\rho = rho)$:

  $$\tau_j \leftarrow (1 - \rho)\ x\ \tau_j, \forall_j \quad \text{(eq. 5)}$$

  where τ_j the pheromone trail intensity for the *j-th* parameter rho (ρ) is the evaporation rate and the symbol $\forall_j$ signifies that this operation is applied "for all parameters."
- Deposition: The pheromone trails are reinforced based on the quality of the best solutions found in the current iteration. In the elitist update strategy used, the *Ne* (*Elite_ants*) solutions with the lowest RMSE values contribute to the pheromone update for each parameter *j*:

  $$\tau_j \leftarrow \tau_j + \sum_{k=1}^{Ne} \frac{Q}{RMSE} \quad \text{(eq. 6)}$$

  where Q is a constant defining the pheromone deposit intensity.
- New Population Construction: A new generation of N_{ants} solutions is constructed using "Parent Selection and Gaussian Sampling".

  Parent Selection: For each new ant, a parent solution X_{parent} is selected based on the q_0 factor. With probability q_0, the global best X_{best} is chosen. With probability $(1 - q_0)$ a parent is chosen via a roulette wheel mechanism, which favors solutions with lower RMSE.

  Gaussian Sampling: A new solution X_{new} is generated by sampling from a Gaussian (Normal) distribution centered on the parent:

  $$X_{new} \sim N(X_{parent}, \Sigma) \quad \text{(eq. 7)}$$

  The standard deviations within the covariance matrix Σ are inversely proportional to the updated pheromone trails τ_j, promoting a finer search around solutions with high pheromone levels.
- Increment and loop: The iteration counter is incremented.

This balance of exploration (via evaporation) and exploitation (via pheromone reinforcement) enables effective navigation of the complex, non-convex PV parameter space.

The ACO flow diagram presetting on Figure 2:

2.3.2 Modifications and Hybridization

The standard ACO framework was enhanced with three strategies to tailor it specifically for the PV parameter extraction problem:

- Reduced Search Space Strategy: To drastically improve computational efficiency and avoid the complexities of a high-dimensional search space, the ACO does not optimize all five parameters of the SDM simultaneously. Instead, the metaheuristic search is focused on the three most influential and interdependent parameters: the diode ideality factor, the series resistance and the shunt resistance. The remaining two parameters—photocurrent (I_{ph}) and diode saturation current (I_s) —are calculated analytically at each evaluation of the objective function, using the experimental values at the open-circuit and short-circuit points (V_{oc} I_{sc}) . This is achieved by first applying the open-circuit ($I_{pv} = 0$, $V_{pv} = V_{oc}$) and short-circuit ($V = 0$, $I_{pv} = I_{sc}$)(Ben said et al., 2024):

$$I_s = \frac{I_{sc} * \left(1 + \frac{R_S}{R_{sh}}\right) - \left(\frac{V_{oc}}{R_{sh}}\right)}{e^{\left(\frac{V_{oc}}{(n*Vt)}\right)} - e^{\frac{(R_S * I_{SC})}{(n)Vt}}} \qquad \text{(eq. 8)}$$

$$I_{ph} = I_{sc} + I_s\left(e^{\frac{R_{S*}I_{SC}}{nVt}} - 1\right) + \frac{R_{S*}I_{SC}}{R_{sh}} \qquad \text{(eq. 9)}$$

For the Double-Diode Model (DDM) this work proposes a novel extension of the reduced search strategy. The 7-parameter problem was reduced to a 4-parameter optimization by assuming $n_1 = n_2 = A$ an effective ideality factor), for reduce de search space and calculating a total saturation current I_s and I_{ph} using (eq. 7) and (eq. 8) (with A replacing n). This total current is then split between the two diodes using a new optimized parameter, *frac* in [0, 1] such that:

$$I_{s1} = frac * Is \qquad \text{(eq. 10)}$$

$$I_{s2} = (1 - frac) \qquad \text{(eq. 11)}$$

with I_{s1} *and* I_{s1} calculated the algorithm uses the eq. 3 to calculate the RMSE

- Hybridization with Local Search: To enhance exploitation and accelerate convergence, the ACO is hybridized with a local search mechanism. At the end of each iteration, the best solution found by the swarm, X_{best}, is subjected to a refinement process. A candidate solution, Xcand, is generated in the neighborhood of th best solution:

  $$Xcand = Xbest + N(0, \sigma_{LS}) \qquad \text{(eq. 12)}$$

  Where $N(0, \sigma_{LS})$ represents a random perturbation vector drawn from a normal distribution with a mean of zero and a small, predefined standard deviation σ_{LS}. If RMSE(Xcand) < RMSE(Xbest), the best solution is updated with the candidate solution, thus fine-tuning the search.

- Anti-Stagnation Mechanism: To ensure robust exploration and prevent the algorithm from getting trapped in local optima, an anti-stagnation strategy was implemented. If the global best solution is not improved for a predefined number of consecutive iterations (*Stagnation_patience*), the pheromone trails are completely reset. This forces the ant colony to abandon the current, potentially suboptimal, search area and encourages a new wave of global exploration, thereby increasing the algorithm's ability to find the true global minimum.

ACO + LOCAL SEARCH + REDUCED SEARCH (ACO-LSR) flow diagram is presenting by de figure 2 – B

2.4 Statistical Performance Metrics

While the RMSE (Equation 4) serves as the objective function guiding the internal search process of the algorithms, a different set of metrics is required to evaluate and compare their overall performance from a statistical standpoint. To ensure a robust and unbiased comparison, each algorithm was executed multiple times independently. The final RMSE values from these runs were then aggregated and analyzed using the following standard statistical metrics:

- Best and Worst RMSE: These metrics indicate the range of performance, showing the best possible solution found and the worst-case outcome across all runs.
- Mean RMSE: Represents the average performance of the algorithm, providing an indication of its general accuracy.
- Standard Deviation (Std. Dev.) of the RMSE**:** This is a crucial metric used to measure the consistency and robustness of an algorithm. A low standard deviation implies that the algorithm consistently converges to solutions similar, indicating high reliability.
- Mean Iterations to Threshold: This metric evaluates the convergence speed and efficiency of each algorithm. It records the average number of iterations required by an algorithm to first achieve an RMSE value below a predefined high-precision threshold, which was set to 5x 10^{-3} in this study.

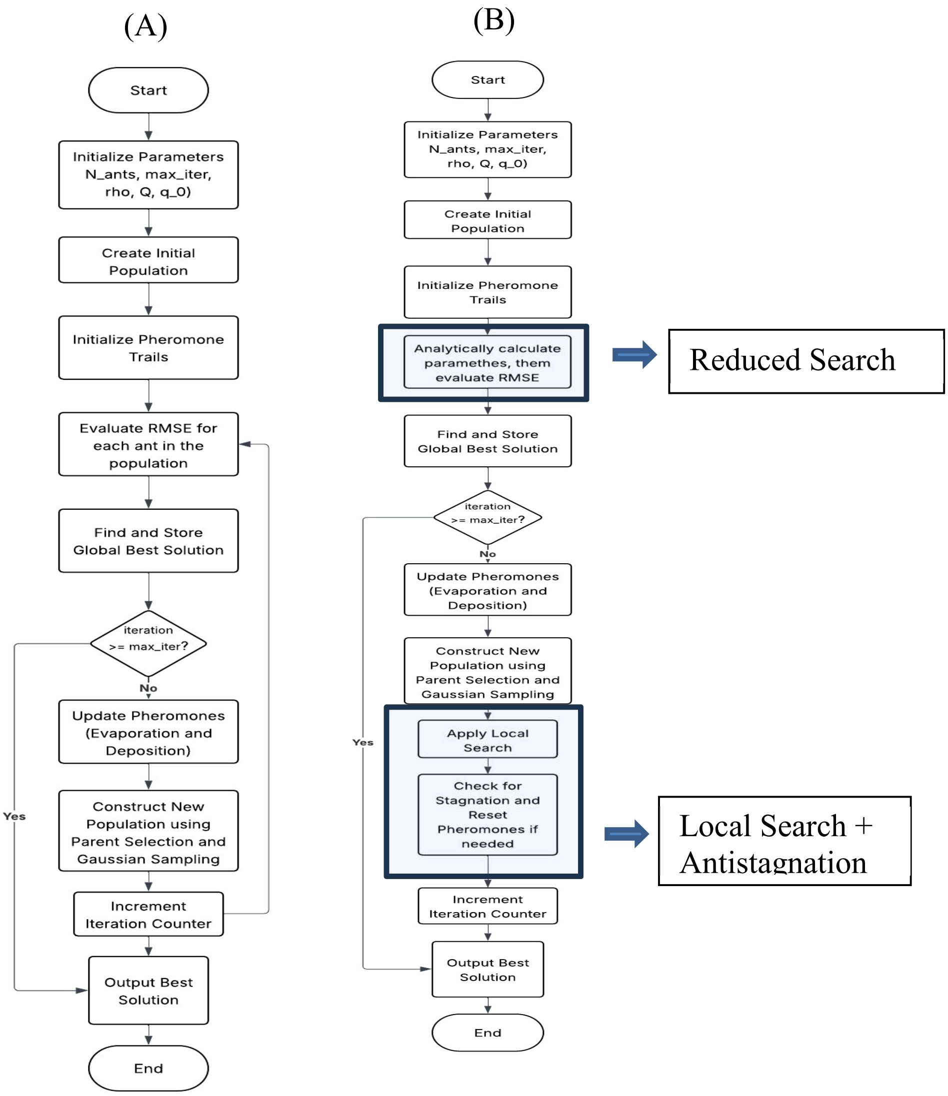

Figure 2 – (A)-ACO flow diagram and (B) - ACO-LSR flow diagram.

2.5 Experimental Setup

To ensure a fair and reproducible comparison, all experiments were conducted under a unified framework.

- Dataset: The validation of the algorithms was performed using a widely recognized experimental dataset from a 57-mm-diameter commercial silicon solar cell (R.T.C. France). The I-V data consists of 26 measurement points collected under an irradiance of 1000 W/m² and a cell temperature of 33 °C. This dataset is frequently used as a benchmark in the literature for parameter extraction problems with the followed vectors (Easwarakhanthan et al., 1986):
- Benchmarking Algorithms: The performance of the proposed ACO-HSR was benchmarked against the author's own standard implementations of three well-established metaheuristic algorithms. The Particle Swarm Optimization (PSO) was implemented based on the original model proposed by (Kennedy and Eberhart, 1995). The Genetic Algorithm (GA) followed the foundational concepts of evolutionary algorithms introduced by (Holland, 1975). Finally, the Simulated Annealing (SA) algorithm was based on the principles described by (Van Laarhoven and Aarts, 1987).
- Implementation and Protocol: All optimization algorithms were implemented in Python 3 within a Jupyter Notebook environment. The post-processing of results and the plotting of I-V were performed in

MATLAB. To guarantee statistical significance, each algorithm was executed 30 times independently for each model.

- Computational Environment: All simulations were carried out on a Dell G15 5511 laptop equipped with an 11th Gen Intel(R) Core(TM) i5-11400H @ 2.70GHz processor and 16 GB of RAM, running on a Windows 11 Home operating system.
- Proposed Algorithm Parameters The parameters for the proposed ACO- LSR algorithm were configured with a population size (Num_ants) of 100 ants and was run for a maximum of 400 iterations (*Max_iter*). The pheromone update mechanism was controlled by an evaporation rate (rho) of 0.5, a deposit intensity (Q) of 100, and an elite pool size (*Elite_ants*) of 3. The ant selection process was guided by an exploration/exploitation factor (q0) of 0.6, and the anti-stagnation mechanism (Stagnation_patience) was set to trigger after 30 iterations without improvement.

This section presents the experimental results in two stages. First, a comparative study is conducted to evaluate the impact of the proposed modifications on the ACO algorithm and justify the selection of the final hybrid model (ACO-LSR). Second, the performance of the selected ACO-LSR is benchmarked against other well-established metaheuristics for both the SDM and DDM problems.

3. Result and discussion

To validate the effectiveness of the proposed architectural enhancements, four distinct versions of the ACO algorithm were tested on the SDM problem over 30 independent runs:

- Standard ACO: The conventional ACO algorithm applied to the full 5-parameter space.
- ACO with Local Search: The standard 5-parameter ACO enhanced with the local search mechanism.
- ACO with Reduced Search: The ACO algorithm applied to the reduced 3-parameter space, without local search.
- ACO-LSR: The proposed final version, combining both the reduced search space and the local search hybridization.

The statistical results of this comparative study are summarized in Table 1.

Table 1 Statistical Results of Final RMSE for the SDM/DDM over 30 Independent Runs.

Algorithm	Best SDM / DDM ($x10^{-2}$)	Mean SDM / DDM ($x10^{-2}$)	Std. Dev. SDM / DDM ($x10^{-2}$)	Mean Iterations to Reach RMSE < $5x10^{-3}$ SDM / DDM
Standard ACO	2.942 / 6.75	8.228 /15.2077	3.466 /4.4276	N/A – N/A
ACO + Local Search	0.1970 /0.2694	0.3784 /0.5599	0.1322 /0.1896	350 – N/A
ACO + Reduced Search	0.2572 /0.7718	0.5792 /1.8332	0.2030 /0.7680	53/379
ACO-LSR	0.1931/0.2777	0.1938 /0.4168	0.0007/0.0156	5/11

The results from the comparative study demonstrate the synergistic effect of the proposed modifications. As observed from Table 1 the Standard ACO performed poorly, failing to converge to a solution within the specified precision threshold (indicated by 'N/A' for Mean Iterations). For the SDM, it presented a high mean RMSE of 8.228×10^{-2} with a standard deviation of 3.466×10^{-2}. Similarly, for the DDM, its mean RMSE was 0.152077 and the standard deviation was 0.044276, clearly indicating high variability and low accuracy.

The addition of either the local search or the reduced search space strategy provided a significant improvement in accuracy and convergence. For instance, the ACO + Local Search variant dramatically reduced the mean RMSE to 3.784×10^{-3} for the SDM and 0.005599 for the DDM. The ACO + Reduced Search variant also showed considerable improvement, achieving a mean RMSE of 5.792×10^{-3} (SDM) and 0.018332 (DDM), with convergence times of 53 and 379 iterations, respectively, to reach the precision threshold.

The combination of both strategies in the ACO-LSR yielded superior performance across all metrics. For the SDM, it achieved the lowest mean RMSE of 1.938 x 10^{-3} and exhibited exceptional robustness with the lowest standard deviation of 7.0 x 10^{-6}, reaching the precision threshold in just 5 iterations. Similarly, for the DDM, it recorded the lowest mean RMSE of 0.004168 and a standard deviation of 0.000156, converging in 11 iterations. This combined approach significantly outperformed all other variants in terms of accuracy, robustness, and convergence speed, thus confirming its selection as the definitive algorithm for the subsequent comparative analysis.

To evaluate the performance of ACO-LSR against other established metaheuristics, a comparative statistical analysis was conducted over 30 independent runs for both the SDM and DDM. The results are summarized in Table 2, Figure 3 and Figure 4.

Table 2 Statistical Results of Final RMSE for the SDM/DDM over 30 Independent Runs.

Algorithm	Best SDM/DDM ($x10^{-3}$)	Mean SDM/DDM ($x10^{-3}$)	Worst SDM/DDM ($x10^{-3}$)	Std. Dev. SDM/DDM (x 10^{-6})	Mean Iterations to Reach RMSE < 5 x 10^{-3} SDM/DDM
ACO-LSR	1.930/2.777	1.936/4.168	1.946/4.423	6.0 /9.0	5/11
PSO	0.9720/2.241	1.342/2.152	1.864/4.807	245 /1190	24/58
GA	0.8170/2.514	1.651/23.32	3.332/22.29	533/444.9	18/43
SA	2.350/2.475	2.350/2.685	52.58/4.907	1279/894	3900/3943

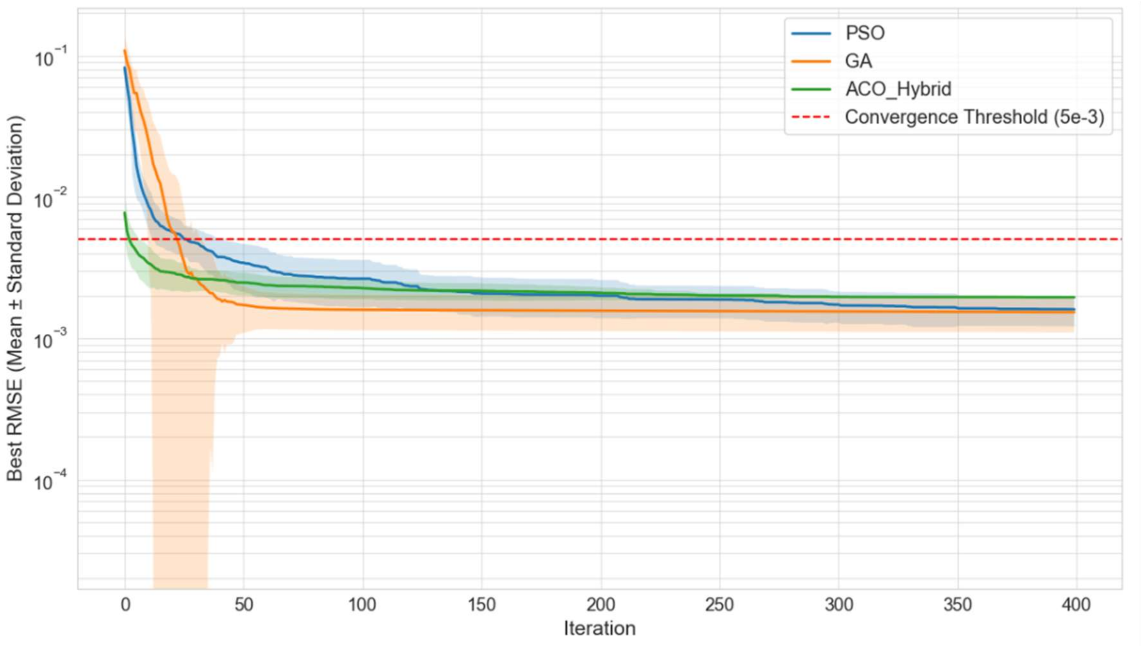

Figure 3- Convergence of the RMSE calculated for the SDM using different algorithms

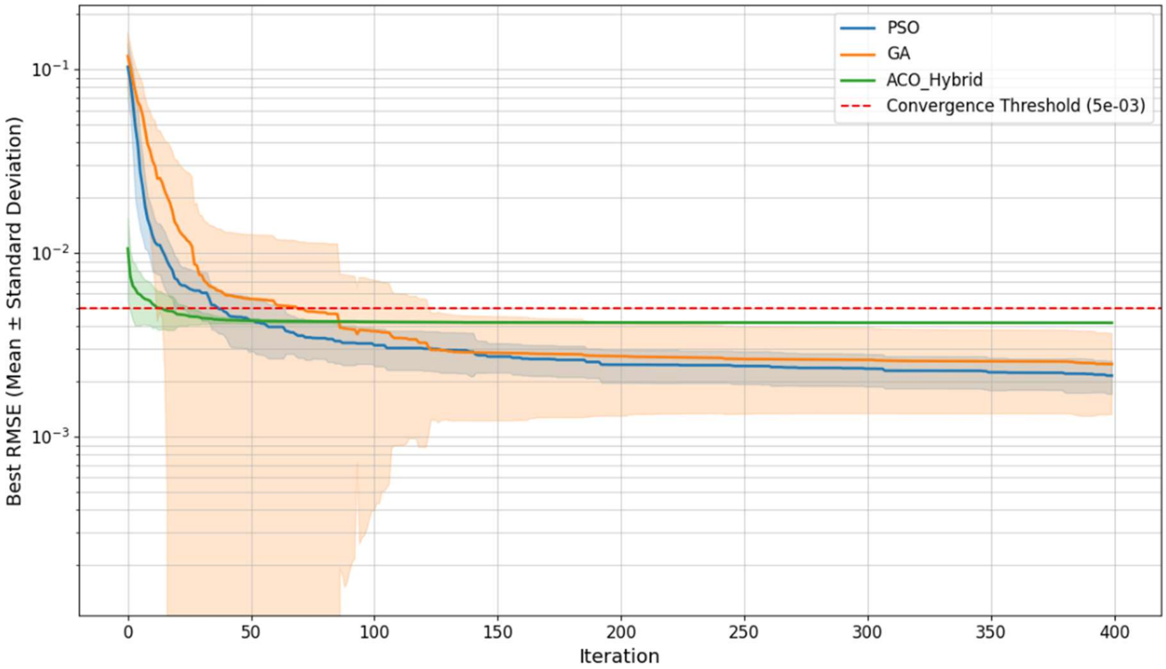

Figure 4- Convergence of the RMSE calculated for the DDM using different algorithms

For both models, the parameters extracted by ACO result in a simulated I-V curve that shows a competitive fit with the experimental data as shown in Figure 5.

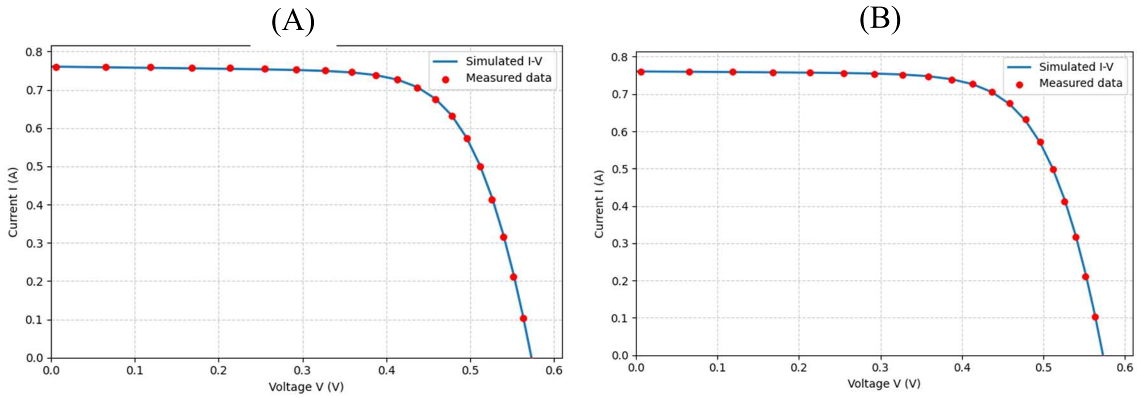

Fig. 5: I-V curve. Dots are experimental values and line is the fitting using (A) SDM and (B)DDM

For the SDM problem (Table 2), while PSO and GA achieved a better mean RMSE on average, their performance was highly variable, evidenced by standard deviations approximately 40 times (for PSO) and 88 times (for GA) larger than that of the proposed ACO variant. In contrast, the proposed method delivered an extremely consistent result in every run, with a standard deviation of only 6.0 x 10^{-6}.

This advantage becomes even more pronounced in the more complex DDM problem (Table 2). While the SA algorithm eventually converges to a competitive mean RMSE (2.685 x 10^{-3}), it is extremely inefficient, requiring an average of nearly 4000 iterations to do so. In contrast, the proposed ACO algorithm is significantly more accurate and reliable than PSO and GA, achieving a mean RMSE approximately 5 times lower and with a standard deviation order of magnitude smaller. This highlights the proposed method's ability to handle increased problem complexity without sacrificing consistency.

Superior efficiency is also represented in the convergence plot in Figure 3 and 4. The SA algorithm was omitted from this figure for clarity, as its convergence to the precision threshold was significantly slower, requiring an average of nearly 4000 iterations for both models (Table 2), which is well beyond the scale of the plot. While other algorithms exhibit a slower convergence, the proposed ACO (green line) rapidly reaches a stable, low-error region. As shown numerically in Table 2 it reached the high-precision threshold of RMSE < 5 x 10^{-3} in an average of 5 (for SDM) and 11 (for DDM) iterations, respectively. This rapid convergence to a near-optimal solution underscores its practical advantage for real-world engineering applications where computational resources and time are constrained.

To further contextualize the performance of the proposed ACO-LSR , its best results are benchmarked against state-of-the-art outcomes reported in recent literature for the same R.T.C. France solar cell dataset. A selection of high-performing and frequently cited algorithms was chosen for this comparison, including the Firefly Algorithm (FA) (Louzazni et al., 2018), Repaired Adaptive Differential Evolution (RADE) (Louzazni et al., 2018), Fitness-Distance Balance-based Stochastic Fractal Search (FDB-SFS) (Bakır, 2023), Enhanced Chaotic Jaya Algorithm (CJAYA) (Premkumar et al., 2021), and other modern methods like Improved Teaching-Learning-Based Optimization (ITLBO) (Li et al., 2019). The comparative results for the Single-Diode Model (SDM) and Double-Diode Model (DDM) are presented in Table 3 and Table 4, respectively.

Table 3 Comparison of ACO with State-of-the-Art Literature for the SDM.

Parameter	ACO-LSR	PSO	GA	SA	FA	TTA-MDEW	FDB-SFS	RADE	CJAYA
Iph (A)	0.7612	0.7608	0.761	0.756	0.7607	0.7607	0.7608	0.7607	0.7607
Is (x10-7A)	2.098	3.266	3.844	6.112	4.324	3.230	3.230	3.230	3.230
n	1.441	1.481	1.459	1.547	1.452	1.481	1.481	1.481	1.481
Rs (Ω)	0.0380	0.0364	0.0327	0.0329	0.0334	0.0363	0.0364	0.0363	0.0363
Rsh (Ω)	53.24	53.71	53.79	57.07	53.40	53.71	53.71	53.71	53.71
RMSE (x10-3)	1.930	0.972	0.817	2.35	0.5138	0.7753	0.986	0.986	0.986
Ref.	Present work	Present work	Present work	Present work	(Louzazni et al., 2018)	(Chermite and Douiri, 2024)	(Bakır, 2023)	(Louzazni et al., 2018)	(Premkumar et al., 2021)

Table 4 Comparison of ACO with State-of-the-Art Literature for the DDM.

Parameter	ACO-LSR	PSO	GA	SA	FA	FDB-SFS	RADE	ITLBO	BHCS
Iph (A)	0.7605	0.7621	0.7603	0.76063	0.7608	0.7608	0.7607	0.7608	0.76078
IS1 (x10-7A)	1.000	6.032	1.0775	9.333	5.911	2.360	2.259	2.260	7.493
IS2(x10-7A)	8.295	2.3147	3.3531	7.1731	2.453	2.740	7.493	7.493	2.259
N1	1.3932	1.580	1.687	1.660	1.0246	1.4678	1.4510	1.4510	2.0000
N2	1.0137	1.587	1.568	1.669	1.3644	1.8899	2.0000	2.0000	1.4510
Rs (Ω)	0.0446	0.0313	0.02993	0.0295	0.0366	0.0365	0.0367	0.0367	0.0367
Rsh (Ω)	53.97	55.441	53.93	58.635	55.04	54.44	55.48	55.48	55.48
RMSE (x10-3)	2.777	2.241	2.514	2.475	0.4548	0.9840	0.9824	0.9824	0.9824
Ref.	Present work	Present work	Present work	Present work	(Louzazni et al., 2018)	(Bakır, 2023)	(Bakır, 2023)	(Li et al., 2019)	(Li et al., 2019)

The comparison with published data reveals that while the ACO-LSR does not achieve the absolute lowest RMSE values reported in the literature, its results remain competitive. A deeper analysis of the parameter values in the tables provides critical insights into the algorithm's performance and the nature of the optimization problem.

For the Single-Diode Model (Table 3), it is noteworthy that the physical parameters extracted by the ACO-LSR I_{ph}, n, R_s and R_{sh} are remarkably similar to those found by state-of-the-art algorithms like FDB-SFS and RADE, even when their final RMSE values differ. For instance, the values for R_s (0.0380) and R_{sh} (53.24) are very close to those reported by RADE (0.0363 and 53.71, respectively). This indicates that the proposed algorithm correctly identifies the near-optimal region in the parameter space, even if other highly tuned methods achieve a marginally better final fit.

This trend changes in the more complex Double-Diode Model (Table 4), which highlights the parameters that are most sensitive to the optimization process. While parameters such as I_{ph}, R_s, and R_{sh} remain relatively consistent across the different algorithms, the diode-specific parameters show significant variation. For example, the ACO-LSR converged to a solution with a second diode saturation current I_{s2} of 8.295 x 10^{-7} A, which is several orders of magnitude smaller than the values found by FA or FDB-SFS (around 2.5 x 10^{-7}A). Similarly, the ideality factors (n_1 and n_2) also vary considerably, with the proposed method finding values of 1.39 and 1.01, while other methods converge to different combinations, such as 1.45 and 2.00. This suggests that I_{s1}, I_{s2}, n_1, *and* n_2 are the most sensitive parameters, and that multiple distinct combinations can yield a competitively low RMSE.

4. Conclusion

This works presented the development and validation of a hybrid Ant Colony Optimization algorithm, enhanced with a local search and a reduced search space strategy for the parameter extraction of single-diode (SDM) and double-diode (DDM) photovoltaic models. The primary objective was to evaluate its performance through a Comparative study and a comparative analysis against established metaheuristics.

The proposed ACO achieved competitive accuracy, obtaining a best-run Root Mean Square Error (RMSE) of 1.930x10^{-3} for the SDM and 2.777 x10^{-3} for the DDM. A comprehensive comparative study confirmed that the combination of both the reduced search space and local search mechanisms was effective, yielding superior performance in accuracy, robustness, and efficiency over the standard ACO or singly-enhanced variants.

The comparative analysis for the SDM, the ACO-LSR exhibited a standard deviation of 6.0 x10^{-6}, a value approximately 40 times smaller than that of PSO, demonstrating exceptional consistency. This advantage was even more pronounced in the more complex DDM problem, where the proposed method reliably converged to a solution (mean RMSE of 4.168 x10^{-3}) while other metaheuristics like PSO and GA struggled to do so under the same computational cost. Furthermore, the ACO reached a high-precision threshold (RMSE < 5 x10^{-3}) in an average of only 5 and 11 iterations for the SDM and DDM, respectively, confirming its superior convergence speed.

In conclusion, the proposed hybrid ACO algorithm proves to be a highly practical and dependable method for PV parameter extraction. While not always achieving the absolute lowest RMSE when compared to the broader literature, its ability to deliver consistent, near-optimal solutions with high efficiency makes it a compelling choice for real-world engineering applications where a balance between accuracy, reliability, and computational cost is paramount. Future work could involve applying this methodology to the three-diode model and extending the analysis to different PV technologies.

5. Acknowledgments

The authors gratefully acknowledge the financial and institutional support from Fundação de Amparo a Ciência e Tecnologia do Estado de Pernambuco (FACEPE) and Conselho Nacional de Desenvolvimento Científico e Tecnológico (CNPq)-Brazilian Agencies (FACEPE BPP-0075-3.05/24). Also, the authors acknowledge the PIBIC scholarship Edital de Iniciação Científica, Tecnológica e Inovação – 2024 (Edital ICTI 2024)

6. References

Bakır, H., 2023. Comparative performance analysis of metaheuristic search algorithms in parameter extraction for various solar cell models. Environmental Challenges 11, 100720.

Ben said, Y., Sakhi, Z., Bennai, M., 2024. An approach for improving parameter extraction in PV solar cell models using metaheuristic algorithms. Energy Systems.

Chermite, C., Douiri, M.R., 2024. Hybrid tiki taka and mean differential evolution based weibull distribution: A comprehensive approach for solar pv modules parameter extraction with newton-raphson optimization. Energy Conversion and Management 314, 118705.

Dorigo, M., Di Caro, G., 1999. Ant colony optimization: a new meta-heuristic. Proceedings of the 1999 Congress on Evolutionary Computation-CEC99, Washington, DC, USA, 6-9 July, pp. 1470–1477.

Easwarakhanthan, T., Bottin, J., Bouhouch, I., Boutrit, C., 1986. Nonlinear Minimization Algorithm for Determining the Solar Cell Parameters with Microcomputers. International Journal of Solar Energy 4, 1–12.

Fahim, S.R., Hasanien, H.M., Turky, R.A., Aleem, S.H.E.A., Ćalasan, M., 2022. A Comprehensive Review of Photovoltaic Modules Models and Algorithms Used in Parameter Extraction. Energies, 15, 8941.

Holland, J.H., 1975. Adaptation in natural and artificial systems: an introductory analysis with applications to biology, control, and artificial intelligence, first ed. University of Michigan Press, Ann Arbor.

Hu, X.-M., Zhang, J., Chung, H.S.-H., Li, Y., Liu, O., 2010. SamACO: variable sampling ant colony optimization algorithm for continuous optimization. IEEE Transactions on Systems, Man, and Cybernetics, Part B: Cybernetics 40(6), 1555–1566.

Ishaque, K., Salam, Z., Taheri, H., 2011. Simple, fast and accurate two-diode model for photovoltaic modules. Solar Energy Materials and Solar Cells 95(2), 586–594.

Kennedy, J., Eberhart, R., 1995. Particle swarm optimization. Proceedings of the ICNN'95-International Conference on Neural Networks, Perth, Australia, 27 November–1 December, pp. 1942–1948.

Li, S., Gong, W., Yan, X., Hu, C., Bai, D., Wang, L., Gao, L., 2019. Parameter extraction of photovoltaic models using an improved teaching-learning-based optimization. Energy Conversion and Management 186, 293-305.

Louzazni, M., Khouya, A., Amechnoue, K., Gandelli, A., Mussetta, M., Crăciunescu, A., 2018. Metaheuristic algorithm for photovoltaic parameters: Comparative study and prediction with a Firefly algorithm. Applied Sciences 8(3), 339.

Ben Messaoud, R., 2020. Extraction of uncertain parameters of double-diode model of a photovoltaic panel using Ant Lion Optimization. SN Applied Sciences 2, 239.

Premkumar, M., Jangir, P., Sowmya, R., Elavarasan, R.M., Kumar, B.S., 2021. Enhanced chaotic jaya algorithm for parameter estimation of photovoltaic cell/modules. ISA Transactions 116, 139-166.

Van Laarhoven, P.J.M., Aarts, E.H.L., 1987. Simulated annealing, in: Van Laarhoven, P.J.M., Aarts, E.H.L., Simulated Annealing: Theory and Applications. Springer, Dordrecht.

Xiong, G., Zhang, J., Shi, D., He, Y., 2018. Parameter extraction of solar photovoltaic models using an improved whale optimization algorithm. Energy Conversion and Management 174, 388-405.